Title

Red Blood Cell Metabolic Responses to Torpor and Arousal in the Hibernator Arctic Ground Squirrel

Journal

Journal of Proteome Research, 18(4)

ISSN

1535-3893

Authors

Gehrke, Sarah
Rice, Sarah
Stefanoni, Davide
et al.

Publication Date

2019-04-05

DOI

10.1021/acs.jproteome.9b00018

Peer reviewed

HHS Public Access

Author manuscript

J Proteome Res. Author manuscript; available in PMC 2020 May 13.

Published in final edited form as:

J Proteome Res. 2019 April 05; 18(4): 1827–1841. doi:10.1021/acs.jproteome.9b00018.

Red Blood Cell Metabolic Responses to Torpor and Arousal in the Hibernator Arctic Ground Squirrel

Sarah Gehrke[†], **Sarah Rice**[‡], **Davide Stefanoni**[†], **Rebecca B. Wilkerson**[†], **Travis Nemkov**[†], **Julie A. Reisz**[†], **Kirk C. Hansen**[†], **Alfredo Lucas**[§], **Pedro Cabrales**[§], **Kelly Drew**[‡], **Angelo D'Alessandro**[*,†]

[†]Department of Biochemistry and Molecular Genetics, University of Colorado Denver − Anschutz Medical Campus, Aurora, Colorado 80045, United States

[‡]Department of Chemistry and Biochemistry, University of Alaska Fairbanks, Fairbanks, Alaska 99775, United States

[§]Department of Bioengineering, University of California San Diego, La Jolla, California 92093, United States

Abstract

Arctic ground squirrels provide a unique model to investigate metabolic responses to hibernation in mammals. During winter months these rodents are exposed to severe hypothermia, prolonged fasting, and hypoxemia. In the light of their role in oxygen transport/off-loading and owing to the absence of nuclei and organelles (and thus de novo protein synthesis capacity), mature red blood cells have evolved metabolic programs to counteract physiological or pathological hypoxemia. However, red blood cell metabolism in hibernation has not yet been investigated. Here we employed targeted and untargeted metabolomics approaches to investigate erythrocyte metabolism during entrance to torpor to arousal, with a high resolution of the intermediate time points. We report that torpor and arousal promote metabolism through glycolysis and pentose phosphate pathway, respectively, consistent with previous models of oxygen-dependent metabolic modulation in mature erythrocytes. Erythrocytes from hibernating squirrels showed up to 100-fold lower levels of biomarkers of reperfusion injury, such as the pro-inflammatory dicarboxylate succinate. Altered tryptophan metabolism during torpor was here correlated to the accumulation of potentially neurotoxic catabolites kynurenine, quinolinate, and picolinate. Arousal was accompanied by alterations of sulfur metabolism, including sudden spikes in a metabolite putatively identified as thiorphan (level 1 confidence) —a potent inhibitor of several metalloproteases that play a crucial

[*]**Corresponding Author:** Tel.: 303-724-0096. angelo.dalessandro@ucdenver.edu.

Author Contributions

SR, KD, AD designed the study. SR and KD performed animal experiments and collected the samples. AD, JAR, KCH, and TN set up the metabolomics platform. SG and DS performed sample extraction. DS performed UHPLC-MS analyses. SG, JAR, and AD analyzed the data. RW, JAR, SG, and AD prepared figures and tables. AL and PC performed rat experiments. AD wrote the first draft of the manuscript, and all the authors contributed critically to the finalization of the paper.

Supporting Information

The Supporting Information is available free of charge on the ACS Publications website at DOI: 10.1021/acs.jproteome.9b00018.

Figures S1−S10 (PDF)

Figure S1 detail (PDF) Figure S3 detail (PDF) Table S1 (XLSX) Table S2 (XLSX)

Notes

The authors declare no competing financial interest.

role in nociception and inflammatory complication to reperfusion secondary to ischemia or hemorrhage. Preliminary studies in rats showed that intravenous injection of thiorphan prior to resuscitation mitigates metabolic and cytokine markers of reperfusion injury, etiological contributors to inflammatory complications after shock.

Graphical Abstract

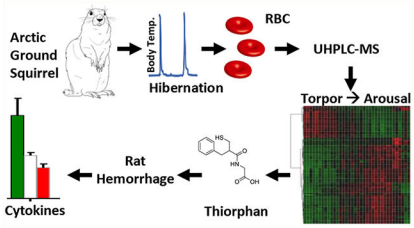

Keywords

sulfur; untargeted metabolomics; tryptophan metabolism

INTRODUCTION

Hibernation in ground squirrels is a paradigmatic example of evolutionary adaptations to extreme environments in mammals. In these hibernating small mammals, a typical circannual life cycle begins with reproduction in spring, followed by growth in summer and accumulation of fat stores during fall—a process that almost doubles the animal body weight—prior to winter months, when hibernation ensues.[1,2] While during spring and summer months hibernating ground squirrels are comparable to normal homeothermic mammals, during winter hibernation months they face prolonged fasting and hetero thermia, i.e., dramatic oscillations in body temperature from ~37 °C to ~0−4 °C or below. Indeed, during winter hibernation months, low body temperature torpor states are interrupted at regular intervals by sudden elevations in metabolic rates through bouts of arousal, accompanied by shivering and nonshivering thermogenesis.

Over the past two decades, discovery-mode omics investigations employing transcriptomics, proteomics, and metabolomics approaches have been exploited to study molecular adaptations to hibernation in the liver, heart, kidney, skeletal muscle, intestine, brown adipose tissue, and plasma from different small mammalian hibernators.[2–15] In particular, extensive exploratory investigations have documented plasma metabolic adaptations in hibernating small mammals,[2,16–18] including a comprehensive description of plasma metabolic phenotypes during entrance into and exit from torpor, as well as early/late and interbout arousal stages.[19] This body of literature has contribute to formulate the hypothesis that interbout arousals, which consume over 70% of winter energy in hibernators,[20] are necessary to replenish circulating levels of metabolic substrates (especially free fatty acids and amino acids) that are consumed by metabolism at low body temperature during torpor.[4,9,12] At the same time, arousal has been shown to promote the removal from the bloodstream of metabolic waste products that accumulate during torpor.[4,9,12]

In arctic ground squirrels (*Spermophilus parryii*) oxygen consumption decreases by >90% during torpor (which results in decreased body temperature, heart and breathing rates), and increases profoundly during arousal to meet sudden metabolic demands for thermogenesis, mostly fueled by oxidation of fat stores accumulated during fall. RBCs—by far the most abundant host cell in the human body[21,22]—play a key role in oxygen transport and off-loading. Though previous studies showed no significant changes in circulating erythrocyte counts, hematocrit, or total hemoglobin between summer stages or winter torpor/arousal cycles in 13-lined ground squirrels,[23] it is worth noting that RBCs are endowed with metabolic signaling cascades that promote oxygen off-loading and tissue oxygenation as a result of systemic hypoxemia. However, none of these studies have addressed RBC metabolism in hibernating mammals. Indeed, RBCs represent a perfect model to investigate metabolism, in that they are devoid of de novo protein synthesis capacity (owing to the lack of nuclei and organelles), while they are characterized by a tight oxygen-dependent metabolic reprogramming. Oxygen dependent metabolic modulation in RBCs is mediated by the interactions of hemoglobin and band 3—the most abundant cytosolic and membrane proteins in mature RBCs, respectively. The N-terminal cytosolic domain of band 3 serves as a docking site for both deoxygenated hemoglobin and glycolytic enzymes (phosphofructokinase, aldolase, and glyceraldehyde 3 phosphate dehydrogenase, GAPDH).[24–26] Under low oxygen tensions, deoxygenated hemoglobin[27] competes with glycolytic enzymes for the same docking site in the N-term of band 3. Deoxyhemoglobin binding to the N-term of band 3 promotes the release into the cytosol (and concomitant activation) of glycolytic enzymes.[28–30] Through this mechanism, hypoxia promotes glycolysis in RBCs, which in turn acidifies the intracellular pH and generates high-energy phosphate compounds (adenosine triphosphate, ATP, and 2,3-diphosphogly cerate, DPG). Intracellular levels of ATP and DPG further stabilize the tense deoxygenated state of hemoglobin and promote oxygen off-loading and tissue oxygenation in response to hypoxia. Under high oxygen tensions, hemoglobin is oxygenated and its binding to band 3 prevented, which results in glycolytic enzymes (inhibitory) binding to band 3 and shifting metabolism toward the pentose phosphate pathway (PPP) —which in turn generates reducing equivalents (e.g., NADPH) to counteract oxidative stress. Here we hypothesize that similar shifts from glycolysis to the PPP occur as a function of torpor and arousal-induced changes in oxygen availability or consumption.

Of note, oxygen-dependent metabolic modulation has been shown to influence system metabolism as a function of circadian rhythms in mammals,[31,32] though no study to date has addressed RBC glycolytic/PPP metabolism during circannual hibernation during torpor and arousal. Similarly, purinergic signaling via the ectonucleotidase CD73, adenosine, adenosine receptors on RBCs, cyclic-AMP and AMPK/PKA has been shown to regulate the binding of key glycolytic enzymes to band 3 and thus the hypoxia-induced switch to glycolysis.[33–35] Strikingly, purinergic signaling has been suggested to participate in induction of torpor through a similar cascade in hibernating small mammals.[36–39]Despite significant advancements in the understanding of the underlying mechanisms of hibernation, the capacity of mammalian hibernators to withstand extreme conditions (e.g., hypothermia, reperfusion injury secondary to ischemia/hemorrhage) is still an unresolved mystery.[16,39–41] Oxygen-dependent metabolic modulation of RBCs has been described in human and mouse

RBCs in response to high-altitude hypoxia,[42] ex vivo incubation under hypoxic/anaerobic conditions,[43] and pathologic hypoxemia in vivo (e.g., following hemorrhagic shock,[44] sickle cell disease,[45] or sepsis[46]). Understanding whether peculiar adaptations exist in RBCs from hibernating mammals could inform on as of yet unappreciated rewiring of metabolic pathways—hitherto unexplored in other mammals—that may underlie arctic ground squirrel resilience to reperfusion upon ischemic/hemorrhagic shock.

In the light of the considerations above, here we performed an extensive (untargeted and targeted) state of the art metabolomics analysis of RBCs from arctic ground squirrels with a longitudinal sampling during torpor and arousal with high time resolution.

MATERIALS AND METHODS

Trapping

Arctic Ground Squirrels (AGS, *Urocitellus parryii)* were trapped early July in the northern Brooks Range, Alaska, 40 miles south of Toolik Field Station (68°38′ N, 149°38′ W) and were transported to Fairbanks, Alaska under permit by the Alaska Department of Fish and Game.

Animals and Ethics Statement

AGS of both sexes were utilized for experiments (full torpor bout sampling experiments: female $n = 2$, male $n = 1$). Body weights ranged from 431 to 674 g. All procedures were performed in accordance with University of Alaska Fairbanks Institutional Animal Care and Use Committee (IACUC).

Husbandry

AGS were housed at ambient temperature (Ta) between 16 and 18 °C at 16L:8D hour light/dark cycle cages until August 15th, when they were moved to cold chambers with Ta of 2 °C at a 4L:20D hour light/dark cycle. Animals were fed approximately 47 g Mazuri Rodent chow (#5663) daily and provided water during the euthermic period. Animals were housed individually in 12′′ × 19′′ × 12′′ stainless steel wire mesh hanging cages over ammonia absorbing corn cob litter. Once animals exhibited robust hibernation behavior, food was withdrawn; animals were placed in polycarbonate cages (8.5′′ × 17′′ × 8.5′′) with shavings, cotton bedding, and gel hydration packets. Polycarbonate cages were placed on receivers linked to a data collection system for core body temperature recording (Data Sciences International, St. Paul, MN, USA).

Surgery

AGS were instrumented with chronic femoral arterial and venous cannulas (3 Fr cannula, Instech Laboratories Inc., Plymouth Meeting, PA, USA) and TA-F40 core body temperature transmitters (Data Sciences International, St. Paul, MN, USA) in July and August. Animals received 1 mg/kg, sc Buprenorphine SR (Zoopharm Pharmacy, Laramie, WY, USA) prior to surgery and 8.88 mg/kg, sc enrofloxacin (Norbrook Laboratories, Newry, BT3T6PU, Co. Down, Northern Ireland, UK) for 3 days postsurgery. Cannula patency was maintained with

a heparin/glycerol locking solution (1:1), and care was taken to remove the locking solution and flush with saline prior to readministering new locking solution.

Experimental Procedure

Experiments took place between late October and early December once animals exhibited multiday torpor bouts. Real time body temperature was recorded at increments of 10 min throughout the hibernation season.

Samples of RBCs were acquired from animals at 12 progressive time points from entrance into torpor, throughout torpor and into full arousal from torpor. Time points were defined as follows: entrance into hibernation (core body temperature (Tb) 10−12 °C), progressive time points throughout the torpor bout (FB1−7, calculated as incremental 10% intervals of the previous torpor bout duration), late torpor (within 80−95% of the previous torpor bout duration), early arousal (2.4−2.5 °C), mid arousal (15−21 °C) and arousal (35−36 °C), representing both homeothermic and hetero thermic phases of hibernation through a torpor/arousal cycle. Natural arousal was verified by monitoring real-time, exponential temperature increases in a nondisturbed animal. Natural arousal was additionally confirmed by visual observation of respiratory rate increase before any sampling took place.

RBC Acquisition

Blood was sampled via arterial line and immediately transferred to nonheparnized microhematocrit tubes (Kimble) and sealed with putty. Blood was centrifuged for 2 min at 4 °C and RBCs were immediately placed on ice. Samples were stored at −80 °C until analysis.

Rat Model of Hemorrhage and Resuscitation

Under approved protocols at the University of California San Diego, Sprague−Dawley rats (Harlan Laboratories, Indian apolis, IN) weighing 200−250 g, were used, with a total of 3 rats per group. The rats were implanted with a left jugular vein catheter and a right femoral artery catheter, and were subject to two different protocols. In both protocols, 50% of the rat's blood volume was removed over 30 min through the arterial line and maintained in hypovolemia for the subsequent 30 min. In protocol 1, rats were treated with an intravenous infusion of thiorphan at 20uL/min to achieve either 1 or 10 μM final plasma concentration (based on the estimated blood volume as determined by 0.07 mL/g of body weight, as previously described[47]), prior to resuscitation to 60% of the extracted blood volume (approximately 30% of the original blood volume) with Hextend at 300uL/min through the venous line. In protocol 2, the thiorphan injection occurred after resuscitation. Each protocol ended with a 60 min recovery period, subsequent to the resuscitation with Hextend. Blood samples were collected through an arterial line and centrifuged according to the same procedure mentioned in the previous section. RBCs and plasma were separated and stored at −80 °C until analysis. Samples were taken at baseline (BL), at 5 and 30 min during shock (SH5 and SH30, respectively), after 5 and 60 min from the beginning of resuscitation (RS5 and RS30, respectively), and immediately after thiorphan injection (TH1 and TH2, for protocols 1 and 2 respectively). A vehicle group was included as a control for the resuscitation treatment. Plasma samples were processed for metabolomics analyses to determine the levels of circulating markers of reperfusion injury succinate, fumarate, and

succinate/fumarate ratios, as well as the levels of circulating cytokines, as previously described.[48]

METABOLOMICS ANALYSES

Extraction

RBC samples were extracted at 1:10 dilution (20 μL in 180 μL) in ice-cold lysis/extraction buffer (methanol: acetonitrile: water 5:3:2 *v*/*v*). The mixture was agitated at 4 °C for 30 min and then centrifuged at 10 000*g* for 15 min at 4 °C. Protein pellets were discarded, while supernatants were stored at −80 °C prior to metabolomics analyses.

Metabolomics Analysis

Metabolomics analyses were performed as previously reported,[49,50] with minor modifications. After sample randomization, 10 μL of extracts were injected into a Thermo Vanquish UHPLC system (San Jose, CA, USA) and resolved on a Kinetex C18 column (150 × 2.1 mm, 1.7 μm, Phenomenex, Torrance, CA, USA) at 450 μL/min through a 5 min gradient from 5 to 95% organic solvent B (mobile phases: A = water, 0.1% formic acid; B = acetonitrile, 0.1% formic acid in positive ion mode or mobile phases: A = 18 mΩH_2O, 1 mM ammonium acetate; B = acetonitrile, 1 mM ammonium acetate for negative ion mode). The UHPLC system was coupled online with a Q Exactive mass spectrometer (Thermo, Bremen, Germany) scanning in Full MS mode or performing data-dependent fragmentation (Top15 ddMS2, for validation) at 70 000 resolution in the 60−900 *m*/*z* range, 4 kV spray voltage, 15 sheath gas and 5 auxiliary gas, operated in negative and then positive ion mode (separate runs). Metabolite assignments were performed using Compound Discoverer (Thermo Fisher, Bremen, Germany) based on intact masses, transition fingerprints (which were used to annotate MS2 spectra and apply FISh scores), against the Chemspider, NIST, BioCyc, LipidMaps and KEGG databases as well as an in-house library of ~1000 standards (Sigma-Aldrich, St. Louis, MO, USA; IROATech, Bolton, MA, USA). Absolute quantitation was performed against stable isotope-labeled internal standards, which have been previously listed and are extensively described. The thiorphan standard was obtained from Sigma-Aldrich.

Data Analysis

Hibernation state differences in metabolite abundances were determined via time-series ANOVA followed by FDR correction for multiple comparisons (MetaboAnalyst 3.0; http://www.metaboanalyst.ca).[51] Partial least-squares-discriminant analysis (PLS-DA) and pathway analyses were performed with MetaboAnalyst 3.0 using merged data from the negative and positive ion mode runs (results for each metabolite from one mode only, e.g., glucose data is from negative ion mode).[52]Hierarchical clustering analyses and plots were obtained with MetaboAnalyst 3.0,[51] GENE E (Broad Institute, MA, USA), Excel (Microsoft, Redmond, CA, USA), and GraphPad Prism5.0 (Prism, La Jolla, CA, USA).

RESULTS

RBCs Undergoes Significant Metabolic Changes during Torpor and Arousal

Untargeted metabolomics analyses were performed on RBCs from arctic ground squirrels during entrance into torpor (Ent), through incremental bouts of torpor (FB1−7, calculated as incremental percentages of the length of torpor bouts at previous cycles), late torpor (LT) and early, middle and full arousal (EA, MA and AR, respectively, Figure 1A). A total of 3927 compounds or chemical formulas were tentatively identified on the basis of intact and fragment mass, against the KEGG, Chemspider, NIST and HMDB databases (Table S1) and analyses through partial least-squares-discriminant analysis (PLS-DA, Figure 1B), Manhattan plots (Figure 1C) and hierarchical clustering analysis (avectorial version is provided in Figure S1, while Figure 1D shows the top 500 significant metabolites by repeated measures ANOVA). PLSDA clearly showed an impact of torpor (PC1, explaining 14.3% of the total variance) and arousal (PC2, 9.4%, Figure 1B). Volcano plots were graphed at each time point in comparison to the Ent stage, with the goal to highlight compounds progressively accumulating or depleting significantly in RBCs during progression through torpor and arousal stages (Figure S2). Of note, significant depletion of >20 compounds was only achieved past the FB7 and LT time points, while significant increases of >50 compounds was observed in RBCs at much earlier stages (FB4, Figure S2).

To validate untargeted metabolomics data, manual spectral annotation was performed against an in-house standard library for 176 metabolites (for which additional information about chromatographic retention times was available) and absolute quantification determined against stable isotope-labeled internal standards for 25 compounds (Table S2). Hierarchical clustering analyses (Figure S3; detailed version of the top ~70 metabolites by repeated measures ANOVA in Figure S4A). and PLS-DA (Figure S4B) were performed on data from semitargeted analyses. Results confirmed progressive changes in metabolites of glycolysis and the PPP (Figure 2), purine and carboxylic acids (Figure S5), fatty acids (Figure S6) during torpor and arousal, though most of these changes in central carbon and nitrogen metabolism were reversed by arousal (see for example the circular distribution of samples in the PLS-DA in Figure S4B), as detailed in the next paragraphs.

Energy and Signaling: From Glycolysis to the PPP, Purine Signaling, Carboxylates and Fatty Acid Sequestration

Though devoid of mitochondria, mammalian RBCs have been reported to respond to hypoxia by shifting glucose oxidation away from the PPP and upregulating glycolysis, a pathway that generates lactate and ATP along with 2,3-DPG via the Rapoport−Luebering shunt. All three compounds contribute to oxygen off-loading by (i) promoting the Bohr effect by acidifying the intracellular pH or (ii) directly stabilizing the tense deoxygenated state of hemoglobin, thus promoting a right shift in the oxygen binding curve of hemoglobin. Here we report that, consistently, torpor-induced hypoxemia is accompanied by alterations in glycolysis, though decreases in all glycolytic intermediates (including DPG) except for pyruvate and lactate were noted during torpor (Figure 2). Of note, increases in hexose and triose phosphates and normalization in the erythrocytic levels of lactate were noted following full arousal. Consistent with the model, torpor (low oxygen stage) decreased

while arousal (high oxygen stage) increased the levels of PPP intermediates and byproducts, with the notable exception of ribose diphosphate, which increased progressively and plateaued at LT (Figure 2).

Purine homeostasis (beyond ATP) and purinergic signaling are intertwined to the oxygen-dependent metabolic modulation of RBCs.[33–35] Increases in adenosine and purine oxidation products (allantoin and allantoate) were noted progressively during torpor and maxed out at LT, right before being normalized by arousal (Figure S5). Purine salvage in mature erythrocytes is incomplete or—as recent tracing data suggest—only minimally active under hypoxic conditions.[52] Simultaneous decreases in RBC aspartate and fumarate during torpor are thus consistent with limited activity of salvage reactions. On the other hand, mitochondria-devoid RBCs are still characterized by cytosolic isoforms of Krebs cycle enzymes, isoforms that participate in the homeostasis of reducing equivalents—as noted by tracing experiments with stable isotope-labeled citrate.[54–55]At the same time, RBC levels of tri and dicarboxylates mirror plasma concentrations in animal models of hemorrhagic shock and resuscitation.[44] While citrate levels plateaued at LT, suggesting scavenging by RBCs during torpor stages, downstream metabolites alpha ketoglutarate (aKG), succinate, fumarate and malate all increased immediately after arousal (Figure S5). Differently from observations in rats suffering from hemorrhagic hypoxemia,[44] RBC levels of succinate in arctic ground squirrels never raised above 8 μM and were normalized immediately after MA (Figure S5). In addition, it is worth noting that 2hydroxyglutarate (2HG) —a marker of hypoxia—progressively decreased during torpor, though aKG/2HG ratios only flipped upon reoxygenation following arousal (Figure S5). Citrate metabolism by cytosolic ATP-citrate lyase results in the generation of acetyl-CoA and oxaloacetate in the mature erythrocyte. In this view, it is worth noting that pantothenate, a CoA precursor, followed overlapping trends with citrate (Figure S6).

In the mature erythrocyte, despite an incomplete fatty acid synthesis and absent fatty acid oxidation, sequestration of free fatty acids through conjugation to carnitines may contribute to maintenance of fatty acid reservoirs.[56] In this view, RBC levels of carnitine-conjugated fatty acids increased progressively during torpor and declined upon arousal, while free fatty acids followed the exact opposite trend, with a sudden spike at MA and immediate decline at full AR (Figure S6).

Progressive accumulation of RBC creatinine and depletion of spermine during torpor (both normalized by arousal) are consistent with ongoing proteolysis and activation of the urea cycle in other tissues than RBCs, and inactivation of polyamine synthesis within the mature RBC during torpor.

RBC Levels of Sulfur Metabolites Were Significantly Impacted by Torpor and Arousal

In light of results suggesting an impairment of glycolysis/PPP homeostasis, we thus focused on redox homeostasis, starting from glutathione metabolism. While increases in the total glutathione pool (both reduced, GSH, and oxidized, GSSG) were noted during FB4-FB7, significant alterations of dehydroascorbate/ascorbate ratios were observed (increases during torpor normalized by arousal, Figure S7). Similarly, glutathione oxidation and turnover products (glutathionylcys-teine and 5-oxoproline) increased transiently during torpor and

decreased upon full-arousal (Figure S7). Glutathione pre cursors cysteine and glutamate (and its precursor proline) remained constant during torpor and increased significantly at MA and full AR (Figure S7), suggesting alterations of one carbon metabolism at these stages. Analyses of metabolites at the cross-roads between one-carbon and sulfur metabolism, including glycine, threonine, *S*-adenosylmethionine, and taurine showed transient increases during torpor to EA, rapidly reversed by MA and full AR (Figure 3). Of note, serine and choline followed trends overlapping those observed for cysteine (Figure 3). On the other hand, methionine (and its oxidation product, methionine-sulfoxide) decreased progressively during torpor and were normalized by MA and full AR (Figure 3). Consistent with the observed alterations in redox homeostasis, torpor induced significant progressive increases in the levels of indole, indoxyl, picolinic acid, quinolinic acid and kynurenine−tryptophan oxidation catabolites whose levels inversely correlated to tryptophan concentrations (Figure S8). Consumption of RBC tryptophan and normalization of tryptophan oxidation catabolites was quickly observed upon full AR (Figure S9).

In light of these results and of similar findings about torpor/arousal-induced oscillations in plasma levels of sulfur metabolites,[19] we performed an enrichment of untargeted metabolomics data for sulfur-containing metabolites (Figure 4A and vectorial version in Figure S9; full list in the second spreadsheet of Table S1). Results indicate a widespread dysregulation of sulfur metabolism, with torpor inducing decreases in thiomorpholine carboxylate (Figure 4B, as validated by high resolution accurate intact mass, Figure 4C, and full annotation of high-resolution tandem mass fragmentation, Figure 4D) —a lanthionine ketimine catabolite (Figure 4E). Similarly, progressive increases in sulfur containing metabolites identified as thiorphan and pentahomomethionine were observed during torpor with sudden spikes and normalization at the MA and full AR stages (Figure 5). Accurate intact mass, extracted ion chromatograms and fully annotated fragmentation spectra are reported for both compounds in Figure 5. Of note, these compounds were the top and second metabolites by fold-change and −log(*p*-value) in volcano plots comparing MA to Ent measurements (Figure 5). Since thiorphan is not—to the best of the authors' knowledge—a naturally occurring compound, (intact and fragment) mass analyses, as well retention times under two different chromatographic conditions were confirmed against a pure synthetic standard (Figure 6).

Intravenous Administration of Thiorphan to Hemorrhaged Rats Prior to Resuscitation Prevents Reperfusion Injury and Increases in Plasma Cytokine Levels

Expanding on the putative identification of thiorphan as a potential metabolite increasing in the RBCs of hibernating squirrels prior to arousal, we tested whether pharmacological administration of thiorphan prior to, or after, resuscitation would mitigate reperfusion injury in hemorrhaged rats. As a result, intravenous administration of thiorphan (both at a dose of 1 and 10 μM—consistent with the levels measured in squirrel RBCs) prior to resuscitation (but not after it) was sufficient to significantly prevent succinate conversion to fumarate (a marker of the reperfusion injury, Figure 7), while other markers of cardiac output, blood gas and metabolic function remained unaltered (Figure S10). Postischemic succinate metabolism to fumarate had been previously linked to the HIF-dependent increase in the levels of plasma cytokines.[57] Of note, thiorphan administration prior to resuscitation prevented the

accumulation of several pro inflammatory cytokines (Figure 7) that have previously been linked to trauma-related inflammatory complications such as acute lung injury.[58,59]

DISCUSSION

Recent advancements in the field of omics technologies have revealed the metabolic complexity of RBCs, an apparently simple cell that compensates for the lack of nuclei and organelles with metabolic signaling cascades which impact oxygen transport and off-loading capacity.[61–63] Such signaling cascades involve high-energy phosphate compounds (ATP and DPG) and their capacity to stabilize the tense, deoxygenated state of hemoglobin to promote oxygen off-loading in response to systemic hypoxemia secondary to physiological (e.g., high altitude[42]), pathological (e.g., hemorrhagic shock,[44] sickle cell[45] disease or sepsis[46]) or iatrogenic (e.g., anaerobic storage[43]) hypoxia. This oxygen-dependent metabolic modulation in RBCs results in increased glycolytic fluxes in response to low oxygen tensions and activation of the PPP to counteract oxidative stress arising in response to high oxygen tensions.[64] Indeed, high oxygen tensions fuel the generation of reactive oxygen species via Fenton and Haber−Weiss chemistry in iron rich RBCs.[65] Oxidative stress can promote a partial blockade of glycolysis and a switch of metabolic flux into the PPP through two main mechanisms: (i) the sequestration of glycolytic enzymes to the N-term of band 3 (a region occupied by deoxygenated hemoglobin under hypoxia)[30,66] and (ii) the oxidation of functional thiols in the active site of rate limiting glycolytic enzymes including GAPDH (at cysteines 152 and 156, and histidine 179).[67,68] Ongoing glycolysis generates increases in intracellular and circulating lactate,[69] a signaling and metabolic mediator in the whole organism, including muscles, liver, brain and cancer cells.[70,71] Consistent with this model, hibernating arctic ground squirrel RBCs are characterized by increases in glycolytic byproducts pyruvate and lactate during torpor, while sudden increases in PPP (as gleaned by the levels of ribose phosphate and isobaric isomers) are observed during arousal. Of note, this coincided with a sudden spike in the metabolism of glutathione precursors (cysteine, glutamate), increased turnover of oxidation products (glutathionyl-cysteine, 5-oxoproline and dehydroascorbate—consistent with classic literature[72]) at the time of arousal. Furthering our analysis of redox biology and sulfur metabolism beyond glutathione, we noted a significant impact of torpor on one-carbon metabolism (with glycine/threonine accumulating during torpor and serine/choline during arousal) —a pathway generating amino acid precursors to the tripeptide glutathione. Of note, one-carbon and sulfur metabolism are intertwined by methionine catabolism, ongoing during torpor in the face of reduced methionine and protein oxidation (e.g., lower levels of methionine sulfoxide and thiomorpholine carboxylate), and normalized to Ent levels upon full arousal.

Torpor and arousal also impacted metabolism of amino acid beyond the aforementioned pathways, consistent with previous studies on plasma and liver in hibernators.[2,9,15,18,19] Of note, RBC levels of other aromatic amino acids (phenylalanine including tyrosine and tryptophan) were consumed during torpor and were normalized during arousal. Catabolism of tryptophan (an essential amino acid that during prolonged starvation may derive from proteolysis) was observed during torpor, with the levels of indoxyl, indole, kynurenine, picolinic acid and quinolic acid increasing in RBCs during torpor, prior to being normalized by arousal. Of note, tryptophan oxidation products kynurenine, quinolinate, and picolinate

have been associated with inflammatory responses,[73] neurotoxicity,[74] and neuroinflammation.[75] Indeed, alterations in RBC levels of tryptophan metabolites have been reported in conditions associated with neurocognitive impairment, such as in Down syndrome.[76] While serotonin—a tryptophan metabolite involved in entrance into hibernation[77]—did not change significantly in our study, altered RBC levels of tryptophan catabolites warrant further mechanistic investigation.

Arousal resulted in the accumulation of metabolites previously associated with oxidative injury secondary to reperfusion after ischemia[79–81] or hemorrhage,[50] among which carboxylic acid alpha-ketoglutarate, succinate, fumarate, and malate. Of note, the levels of these metabolites were up to 100 fold lower than those measured in plasma and RBCs from hemorrhaged rats, pigs, macaques[82,83] and trauma patients, suggestive that the generation of these potentially harmful metabolites, though not completely ablated, is substantially decreased in the hibernator arctic ground squirrel—consistent with previous studies.[16] These metabolites have been previously associated with purine salvage[79–81] (partially active in the mature erythrocyte under hypoxia[52]—see allantoin in the present study) in response to reperfusion injury, when they mediate pro-inflammatory responses driving some of the most critical sequelae to trauma and hemorrhage (e.g., acute lung injury).[57,84] Though devoid of mitochondria, RBCs can uptake, sequester, and metabolize some of these pro inflammatory di/tricarboxylates under hypoxic conditions.[85] Similarly, RBCs can store (via carintine conjugation) and release fatty acids (through active phospholipases and noncanonical redox sensitive lipases such as peroxiredoxin6), a phenomenon that contributes to RBC membrane lipid composition and thus fluidity and deformability.[56] While some free and carnitine-conjugated fatty acids increased progressively during torpor—a marker of ongoing lipolysis and fatty acid sequestration inside the RBCs—sudden spikes in polyunsaturated fatty acids and bile acids were noted during middle arousal. Of note, increases in conjugated bile-acids in RBCs has been noted in inflammatory conditions linked to neurocognitive impairment (e.g., Down syndrome[76]) and may underlie a linkage between reperfusion damage to the liver and the microbiome—responsible for the deconjugation (of taurine) in higher mammals.[86]

Notably, sulfur-containing methionine metabolites SAM and taurine followed trends comparable to tryptophan catabolites, with progressive increases observed during torpor and sudden depletions at arousal. These trends are consistent with what was observed in the plasma of another small mammal hibernator, 13-lined ground squirrels, where this cascade was associated with the potential generation of hydrogen sulfide right before arousal. Generation of hydrogen sulfide could indeed contribute to the innate protection to reperfusion injury observed in these hibernators, since H_2S would inhibit complex IV and thus prevent mitochondrial uncoupling and generation of reactive oxygen species during arousal.[19] Treatment of nonhibernating mammals like mice with H_2S induces a hibernation-like state,[87] though these findings have not yet been recapitulated in the intensive care setting.[88–91] Supported by the most extensive untargeted metabolomics analysis of a biological matrix in hibernating mammals to date, we identified an impact of torpor and arousal on the levels of ~3925 sulfur-containing molecules tentatively identified on the basis of accurate intact mass and fragmentation fingerprints against bioinformatics compound libraries. For example, minor progressive increases in pentahomomethionine were noted

during torpor, followed by a sudden spike during middle arousal followed by normalization after full arousal. Of note, this metabolite may derive from catabolism of glucosinolate reservoirs that the squirrel accumulates in late fall with its diet. Pentahomomethionine is a sulfur-containing precursor to antioxidant glucosinolates, whose synthesis lies at the cross roads of tryptophan, tyrosine and sulfur metabolism—three of the main pathways significantly impacted by arousal in this study.[92] Further validation against a commercially available standard (retention time, intact mass, and fragmentation profiles) was performed for a feature putatively identified as thiorphan, the most significant metabolite (log2MAvsEnt Fold Change: 9.3; Adjusted −log(*p*-value)MavsEnt: 2.3×10^{-11}). Identification of thiorphan (level 1 of confidence[93]) was puzzling at first, since to the best of the authors' knowledge thiorphan is not a naturally occurring compound. However, thiorphan, also known as 3-mercapto-2-benzylpropanoylgly cine, could be theoretically explained as a product of proteolytic cleavage of oxidized tyrosines cross-linked with the cysteinyl-glycine moiety of glutathione. Alternatively, thiorphan synthesis could be explained by condensation of the cysteinyl-glycine (also naturally occurring dipeptide) with phenyl-acetate—a byproduct of phenylalanine catabolism and a substrate for *E. coli* and bacterial metabolism in the gut.[94] Though caution is advised and further studies will be necessary to validate this observation in plasma and other organs from hibernating arctic ground squirrels and other hibernators, it is interesting to note that thiorphan is a potent inhibitor of several metalloproteases and peptidases that are central to reperfusion injury-mediated damage. Indeed, intravenous injection of thiorphan in healthy mice is sufficient to induce increases in body temperature and metabolic rate through inhibition of enkephalinases[95] (consistent with its levels peaking during middle arousal in our study). Also, thiorphan inhibits proteolysis mediated by bacterial thermolysin in response to temperature increases.[96] Thiorphan is an inhibitor of matrix metalloproteases (MMPs), including MMP7 (matrilysin),[97] which plays a critical role in mediating systemic inflammatory responses through the generation of chemokines derived from digestion of extracellular matrix components (e.g., collagen) and subsequent neutrophil activation mediated by the mesenteric lymph following hemorrhagic shock and resuscitation.[98] By inhibiting digestion of extracellular matrix components, thiorphan may play a protective role in lung and gut leak promoting neutrophil infiltration and microbiome translocation, respectively, following ischemic/hemorrhagic injury and reperfusion.[99,100] Finally, by inhibiting enkephalinases, thiorphan has a strong analgesic activity by disrupting nociceptive signaling.[101] Of note, endogenous opioids mediate analgesia to immobilization in vertebrate animals and inhibition of enkephalinases by thiorphan is a positive regulator of analgesic responses.[102] Preliminarily, we adopted a rodent model of hemorrhagic shock where thiorphan was injected prior to or after resuscitation. The hemorrhage in this model is sufficiently severe to induce general ischemia without provoking cardiovascular collapse. As a result, thiorphan injection (at concentrations consistent to those determined in squirrel RBCs) prior to resuscitation was sufficient to prevent succinate conversion to fumarate, a metabolic marker of reperfusion injury.[78,79,103] Since this metabolic phenomenon had been linked to inflammatory complications mediated by plasma cytokine levels,[57] we noted that 1 μM levels of circulating thiorphan was sufficient to prevent increases in plasma pro-inflammatory cytokines upon resuscitation. However, thiorphan did not improve other measurements of cardiac function, blood gas levels and metabolism or ion homeostasis, but

prevented mortality that is usually observed in rats with lactate levels ~15 mM. Future interventional studies could be designed to test whether thiorphan administration could recapitulate the resistance to reperfusion injury observed in the hibernator investigated in this study.

CONCLUSION

Here we report the first comprehensive metabolic profiling of RBCs from arctic ground squirrels with a highly time-resolved progression from entrance into torpor to arousal during hibernation. The rationale behind this study is based on the appreciation that (i) hibernation corresponds to a prolonged period of systemic hypoxemia and hypothermia, and (ii) RBC metabolism responds to physiological and pathological hypoxemia in a way that promotes glycolysis to generate ATP/DPG and thus oxygen off-loading. Consistent with the hypothesis of ongoing oxygen-dependent metabolic modulation in RBCs from hibernating arctic ground squirrels, increased glycolysis was noted until late torpor, while early arousal corresponded to a sudden accumulation of PPP byproducts. Results confirm and expand on previous evidence in plasma about a key role for torpor and arousal in modulating amino acid metabolism. In this view, we report for the first time that torpor and arousal impact amino acid catabolites of tryptophan and sulfur-containing compounds with well establish neurologic/inflammatory function. Through a combination of targeted and untargeted metabolomics approaches we quantified a series of biomarkers of ischemic/hemorrhagic hypoxia (including carboxylic acids such as succinate) and correlated these measurements to alterations in sulfur metabolism. As a result, we report for the first time the putative identification of thiorphan in RBCs from hibernating squirrels, a chemical with potent inhibitory activity toward a series of metalloproteases/metallopeptidases that are well established mediators of inflammatory sequelae to reperfusion injury and nociception. Preliminarily, we show that intravenous injection of thiorphan in hemorrhaged rats is sufficient to mitigate the reperfusion injury driven by resuscitation, as gleaned by measurements of metabolic markers of reperfusion injury (e.g., succinate levels and fumarate/succinate ratios) and circulating levels of pro inflammatory cytokines. Further studies will be necessary to further validate this finding in other tissues and biofluids from arctic ground squirrels and other hibernators.

Supplementary Material

Refer to Web version on PubMed Central for supplementary material.

ACKNOWLEDGMENTS

AD received research support from the Boettcher Foundation (Webb-Waring Early Career Grant—grant cycle 2017). KD received research support from NSF IOS grant 1258179. KD and SR received research support from NIH P20GM103395. The content is solely the responsibility of the authors and does not necessarily reflect the official views of the NIH.

REFERENCES

(1). Carey HV; Andrews MT; Martin SL Mammalian Hibernation: Cellular and Molecular Responses to Depressed Metabolism and Low Temperature. Physiol. Rev 2003, 83 (4), 1153–1181. [PubMed: 14506303]

(2). Epperson LE; Karimpour-Fard A; Hunter LE; Martin SL Metabolic Cycles in a Circannual Hibernator. Physiol. Genomics 2011, 43 (13), 799–807. [PubMed: 21540299]

(3). Hindle AG; Karimpour-Fard A; Epperson LE; Hunter LE; Martin SL Skeletal Muscle Proteomics: Carbohydrate Metabolism Oscillates with Seasonal and Torpor-Arousal Physiology of Hibernation. Am. J. Physiol. Regul. Integr. Comp. Physiol 2011, 301(5), R1440–1452. [PubMed: 21865542]

(4). Epperson LE; Rose JC; Carey HV; Martin SL Seasonal Proteomic Changes Reveal Molecular Adaptations to Preserve and Replenish Liver Proteins during Ground Squirrel Hibernation. Am. J. Physiol. Regul. Integr. Comp. Physiol 2010, 298 (2), R329–340. [PubMed: 19923364]

(5). Williams DR; Epperson LE; Li W; Hughes MA; Taylor R; Rogers J; Martin SL; Cossins AR; Gracey AY Seasonally Hibernating Phenotype Assessed through Transcript Screening. Physiol. Genomics 2006, 24 (1), 13–22.

(6). Rose JC; Epperson LE; Carey HV; Martin SL Seasonal Liver Protein Differences in a Hibernator Revealed by Quantitative Proteomics Using Whole Animal Isotopic Labeling. Comp. Biochem. Physiol., Part D: Genomics Proteomics 2011, 6 (2), 163–170. [PubMed: 21481655]

(7). Epperson LE; Martin SL Quantitative Assessment of Ground Squirrel MRNA Levels in Multiple Stages of Hibernation. Physiol. Genomics 2002, 10 (2), 93–102. [PubMed: 12181366]

(8). Epperson LE; Dahl TA; Martin SL Quantitative Analysis of Liver Protein Expression during Hibernation in the Golden Mantled Ground Squirrel. Mol. Cell. Proteomics 2004, 3 (9), 920–933. [PubMed: 15266006]

(9). Serkova NJ; Rose JC; Epperson LE; Carey HV; Martin SL Quantitative Analysis of Liver Metabolites in Three Stages of the Circannual Hibernation Cycle in 13-Lined Ground Squirrels by NMR. Physiol. Genomics 2007, 31 (1), 15–24. [PubMed: 17536023]

(10). Martin SL; Epperson LE; Rose JC; Kurtz CC; Ané C; Carey HV. Proteomic Analysis of the Winter-Protected Phenotype of Hibernating Ground Squirrel Intestine. Am. J. Physiol. Regul. Integr. Comp. Physiol 2008, 295 (1), R316–328. [PubMed: 18434441]

(11). Hindle AG; Grabek KR; Epperson LE; Karimpour-Fard A; Martin SL Metabolic Changes Associated with the Long Winter Fast Dominate the Liver Proteome in 13-Lined Ground Squirrels. Physiol. Genomics 2014, 46 (10), 348–361. [PubMed: 24642758]

(12). Jani A; Orlicky DJ; Karimpour-Fard A; Epperson LE; Russell RL; Hunter LE; Martin SL Kidney Proteome Changes Provide Evidence for a Dynamic Metabolism and Regional Redistribution of Plasma Proteins during Torpor-Arousal Cycles of Hibernation. Physiol. Genomics 2012, 44 (14), 717–727. [PubMed: 22643061]

(13). Hindle AG; Martin SL Intrinsic Circannual Regulation of Brown Adipose Tissue Form and Function in Tune with Hibernation. Am. J. Physiol. Endocrinol. Metab 2014, 306 (3), E284–299. [PubMed: 24326419]

(14). Hindle AG; Martin SL Cytoskeletal Regulation Dominates Temperature-Sensitive Proteomic Changes of Hibernation in Fore brain of 13-Lined Ground Squirrels. PLoS One 2013, 8 (8), No. e71627.

(15). Nelson CJ; Otis JP; Martin SL; Carey HV Analysis of the Hibernation Cycle Using LC-MS-Based Metabolomics in Ground Squirrel Liver. Physiol. Genomics 2009, 37 (1), 43–51. [PubMed: 19106184]

(16). Bogren LK; Murphy CJ; Johnston EL; Sinha N; Serkova NJ; Drew KL 1H-NMR Metabolomic Biomarkers of Poor Outcome after Hemorrhagic Shock Are Absent in Hibernators. PLoS One 2014, 9 (9), No. e107493.

(17). Klain GJ; Whitten BK Plasma Free Amino Acids in Hibernation and Arousal. Comp. Biochem. Physiol 1968, 27 (2), 617− 619. [PubMed: 5758389]

(18). Nelson CJ; Otis JP; Carey HV Global Analysis of Circulating Metabolites in Hibernating Ground Squirrels. Comp. Biochem. Physiol., Part D: Genomics Proteomics 2010, 5 (4), 265–273. [PubMed: 20728417]

(19). D'Alessandro A; Nemkov T; Bogren LK; Martin SL; Hansen KC Comfortably Numb and Back: Plasma Metabolomics Reveals Biochemical Adaptations in the Hibernating 13-Lined Ground Squirrel. J. Proteome Res 2017, 16 (2), 958–969. [PubMed: 27991798]

(20). Heldmaier G; Ortmann S; Elvert R Natural Hypometabolism during Hibernation and Daily Torpor in Mammals. Respir. Physiol. Neurobiol 2004, 141 (3), 317–329. [PubMed: 15288602]

(21). Bianconi E; Piovesan A; Facchin F; Beraudi A; Casadei R; Frabetti F; Vitale L; Pelleri MC; Tassani S; Piva F; et al. An Estimation of the Number of Cells in the Human Body. Ann. Hum. Biol 2013, 40 (6), 463–471. [PubMed: 23829164]

(22). Sender R; Fuchs S; Milo R Revised Estimates for the Number of Human and Bacteria Cells in the Body. PLoS Biol. 2016, 14 (8), No. e1002533.

(23). Cooper ST; Sell SS; Fahrenkrog M; Wilkinson K; Howard DR; Bergen H; Cruz E; Cash SE; Andrews MT; Hampton M Effects of Hibernation on Bone Marrow Transcriptome in Thirteen-Lined Ground Squirrels. Physiol. Genomics 2016, 48 (7), 513–525. [PubMed: 27207617]

(24). D'Alessandro A; Nemkov T; Sun K; Liu H; Song A; Monte AA; Subudhi AW; Lovering AT; Dvorkin D; Julian CG; et al. AltitudeOmics: Red Blood Cell Metabolic Adaptation to High Altitude Hypoxia. J. Proteome Res 2016, 15 (10), 3883–3895. [PubMed: 27646145]

(25). Chu H; Breite A; Ciraolo P; Franco RS; Low PS Characterization of the Deoxyhemoglobin Binding Site on Human Erythrocyte Band 3: Implications for O2 Regulation of Erythrocyte Properties. Blood 2008, 111 (2), 932–938. [PubMed: 17942752]

(26). Chu H; McKenna MM; Krump NA; Zheng S; Mendelsohn L; Thein SL; Garrett LJ; Bodine DM; Low PS Reversible Binding of Hemoglobin to Band 3 Constitutes the Molecular Switch That Mediates O2 Regulation of Erythrocyte Properties. Blood 2016, 128 (23), 2708–2716. [PubMed: 27688804]

(27). Harrison ML; Rathinavelu P; Arese P; Geahlen RL; Low PS Role of Band 3 Tyrosine Phosphorylation in the Regulation of Erythrocyte Glycolysis. J. Biol. Chem 1991, 266 (7), 4106–4111. [PubMed: 1705546]

(28). Campanella ME; Chu H; Wandersee NJ; Peters LL; Mohandas N; Gilligan DM; Low PS Characterization of Glycolytic Enzyme Interactions with Murine Erythrocyte Membranes in Wild-Type and Membrane Protein Knockout Mice. Blood 2008, 112 (9), 3900–3906. [PubMed: 18698006]

(29). Chu H; Low PS Mapping of Glycolytic Enzyme-Binding Sites on Human Erythrocyte Band 3. Biochem. J 2006, 400 (1), 143− 151. [PubMed: 16836485]

(30). Low PS; Rathinavelu P; Harrison ML Regulation of Glycolysis via Reversible Enzyme Binding to the Membrane Protein, Band 3. J. Biol. Chem 1993, 268 (20), 14627–14631. [PubMed: 8325839]

(31). Cho C-S; Yoon HJ; Kim JY; Woo HA; Rhee SG Circadian Rhythm of Hyperoxidized Peroxiredoxin II Is Determined by Hemoglobin Autoxidation and the 20S Proteasome in Red Blood Cells. Proc. Natl. Acad. Sci. U. S. A 2014, 111 (33), 12043–12048. [PubMed: 25092340]

(32). O'Neill JS; Reddy AB Circadian Clocks in Human Red Blood Cells. Nature 2011, 469 (7331), 498–503. [PubMed: 21270888]

(33). Liu H; Zhang Y; Wu H; D'Alessandro A; Yegutkin GG; Song A; Sun K; Li J; Cheng N-Y; Huang A; et al. Beneficial Role of Erythrocyte Adenosine A2B Receptor-Mediated AMP Activated Protein Kinase Activation in High-Altitude Hypoxia. Circulation 2016, 134 (5), 405–421. [PubMed: 27482003]

(34). Sun K; Zhang Y; D'Alessandro A; Nemkov T; Song A; Wu H; Liu H; Adebiyi M; Huang A; Wen YE Sphingosine-1 Phosphate Promotes Erythrocyte Glycolysis and Oxygen Release for Adaptation to High-Altitude Hypoxia. Nat. Commun 2016, DOI: 10.1038/ncomms12086.

(35). Song A; Zhang Y; Han L; Yegutkin GG; Liu H; Sun K; D'Alessandro A; Li J; Karmouty-Quintana H; Iriyama T Erythrocytes Retain Hypoxic Adenosine Response for Faster Acclimatization upon Re-Ascent. Nat. Commun 2017, 8, 14108. [PubMed: 28169986]

(36). Tupone D; Madden CJ; Morrison SF Central Activation of the A1 Adenosine Receptor (A1AR) Induces a Hypothermic, Torpor-Like State in the Rat. J. Neurosci 2013, 33 (36), 14512− 14525. [PubMed: 24005302]

(37). Zhao Z; Van Oort A; Tao Z; O'Brien WG; Lee CC Metabolite Profiling of 5′-AMP-Induced Hypometabolism. Metab- olomics 2014, 10 (1), 63–76.

(38). Daniels IS; Zhang J; O'Brien WG; Tao Z; Miki T; Zhao Z; Blackburn MR; Lee CC A Role of Erythrocytes in Adenosine Monophosphate Initiation of Hypometabolism in Mammals. J. Biol. Chem 2010, 285 (27), 20716–20723. [PubMed: 20430891]

(39). Bogren LK; Olson JM; Carpluk J; Moore JM; Drew KL Resistance to Systemic Inflammation and Multi Organ Damage after Global Ischemia/Reperfusion in the Arctic Ground Squirrel. PLoS One 2014, 9 (4), No. e94225.

(40). Drew KL; Rice ME; Kuhn TB; Smith MA Neuroprotective Adaptations in Hibernation: Therapeutic Implications for Ischemia-Reperfusion, Traumatic Brain Injury and Neuro degenerative Diseases. Free Radical Biol. Med 2001, 31 (5), 563–573. [PubMed: 11522441]

(41). Lindell SL; Klahn SL; Piazza TM; Mangino MJ; Torrealba JR; Southard JH; Carey HV Natural Resistance to Liver Cold Ischemia-Reperfusion Injury Associated with the Hibernation Phenotype. Am. J. Physiol. Gastrointest. Liver Physiol 2005, 288 (3), G473–480. [PubMed: 15701622]

(42). D'Alessandro A; Nemkov T; Sun K; Liu H; Song A; Monte AA; Subudhi AW; Lovering AT; Dvorkin D; Julian CG; et al. AltitudeOmics: Red Blood Cell Metabolic Adaptation to High Altitude Hypoxia. J. Proteome Res 2016, 15 (10), 3883–3895. [PubMed: 27646145]

(43). Reisz JA; Wither MJ; Dzieciatkowska M; Nemkov T; Issaian A; Yoshida T; Dunham AJ; Hill RC; Hansen KC; D'Alessandro A Oxidative Modifications of Glyceraldehyde 3 Phosphate Dehydrogenase Regulate Metabolic Reprogramming of Stored Red Blood Cells. Blood 2016, 128 (12), e32–42. [PubMed: 27405778]

(44). Reisz JA; Slaughter AL; Culp-Hill R; Moore EE; Silliman CC; Fragoso M; Peltz ED; Hansen KC; Banerjee A; D'Alessandro A Red Blood Cells in Hemorrhagic Shock: A Critical Role for Glutaminolysis in Fueling Alanine Transamination in Rats. Blood Adv 2017, 1 (17), 1296–1305. [PubMed: 29296771]

(45). Sun K; D'Alessandro A; Ahmed MH; Zhang Y; Song A; Ko T-P; Nemkov T; Reisz JA; Wu H; Adebiyi M Structural and Functional Insight of Sphingosine 1-Phosphate-Mediated Pathogenic Metabolic Reprogramming in Sickle Cell Disease. Sci. Rep 2017, DOI: 10.1038/s41598-017-13667-8.

(46). Bateman RM; Sharpe MD; Singer M; Ellis CG The Effect of Sepsis on the Erythrocyte. Int. J. Mol. Sci 2017, 18 (9), 1932.

(47). Slaughter AL; D'Alessandro A; Moore EE; Banerjee A; Silliman CC; Hansen KC; Reisz JA; Fragoso M; Wither MJ; Bacon A; et al. Glutamine Metabolism Drives Succinate Accumulation in Plasma and the Lung during Hemorrhagic Shock. J. Trauma Acute Care Surg 2016, 81 (6), 1012–1019. [PubMed: 27602903]

(48). Nachuraju P; Friedman AJ; Friedman JM; Cabrales P Exogenous Nitric Oxide Prevents Cardiovascular Collapse during Hemorrhagic Shock. Resuscitation 2011, 82 (5), 607–613. [PubMed: 21342744]

(49). D'Alessandro A; Nemkov T; Kelher M; West FB; Schwindt RK; Banerjee A; Moore EE; Silliman CC; Hansen KC Routine Storage of Red Blood Cell (RBC) Units in Additive Solution-3: A Comprehensive Investigation of the RBC Metabolome. Transfusion 2015, 55 (6), 1155–1168. [PubMed: 25556331]

(50). D'Alessandro A; Moore HB; Moore EE; Wither M; Nemkov T; Gonzalez E; Slaughter A; Fragoso M; Hansen KC; Silliman CC; et al. Early Hemorrhage Triggers Metabolic Responses That Build up during Prolonged Shock. Am. J. Physiol. Regul. Integr. Comp. Physiol 2015, 308 (12), R1034–1044. [PubMed: 25876652]

(51). Xia J; Sinelnikov IV; Han B; Wishart DS MetaboAnalyst3.0—Making Metabolomics More Meaningful. Nucleic Acids Res. 2015, 43, gkv380.

(52). Nemkov T; Sun K; Reisz JA; Song A; Yoshida T; Dunham A; Wither MJ; Francis RO; Roach RC; Dzieciatkowska M; et al. Hypoxia Modulates the Purine Salvage Pathway and Decreases

Red Blood Cell and Supernatant Levels of Hypoxanthine during Refrigerated Storage. Haematologica 2018, 103(2), 361–372. [PubMed: 29079593]

(53). D'Alessandro A; Nemkov T; Yoshida T; Bordbar A; Palsson BO; Hansen KC Citrate Metabolism in Red Blood Cells Stored in Additive Solution-3. Transfusion 2017, 57 (2), 325–336. [PubMed: 27813142]

(54). Rolfsson Ó; Sigurjonsson ÓE; Magnusdottir M; Johannsson F; Paglia G; Gudhmundsson S; Bordbar A; Palsson S; BrynjoÍfsson S; Gudhmundsson S; et al. Metabolomics Comparison of Red Cells Stored in Four Additive Solutions Reveals Differences in Citrate Anticoagulant Permeability and Metabolism. Vox Sang. 2017, 112 (4), 326–335. [PubMed: 28370161]

(55). Bordbar A; Yurkovich JT; Paglia G; Rolfsson O; Sigurjonsson ÓE; Palsson BO. Elucidating Dynamic Metabolic Physiology through Network Integration of Quantitative Time Course Metabolomics. Sci. Rep 2017, 7, 46249. [PubMed: 28387366]

(56). Nakano T; Wada Y; Matsumura S Membrane Lipid Components Associated with Increased Filterability of Erythrocytes from Long-Distance Runners. Clin. Hemorheol. Microcirc 2001, 24(2), 85–92. [PubMed: 11381183]

(57). Tannahill GM; Curtis AM; Adamik J; Palsson McDermott EM; McGettrick AF; Goel G; Frezza C; Bernard NJ; Kelly B; Foley NH; et al. Succinate Is an Inflammatory Signal That Induces IL-1β through HIF-1α. Nature 2013, 496 (7444), 238–242. [PubMed: 23535595]

(58). Cross LJM; Matthay MA Biomarkers in Acute Lung Injury: Insights into the Pathogenesis of Acute Lung Injury. Crit. Care Clin 2011, 27 (2), 355–377. [PubMed: 21440206]

(59). Dolinay T; Kim YS; Howrylak J; Hunninghake GM; An CH; Fredenburgh L; Massaro AF; Rogers A; Gazourian L; Nakahira K; et al. Inflammasome-Regulated Cytokines Are Critical Mediators of Acute Lung Injury. Am. J. Respir. Crit. Care Med 2012, 185 (11), 1225–1234. [PubMed: 22461369]

(60). D'Alessandro A; Dzieciatkowska M; Nemkov T; Hansen KC Red Blood Cell Proteomics Update: Is There More to Discover? Blood Transfus. 2017, 15 (2), 182–187. [PubMed: 28263177]

(61). Bryk AH; Wisniewski JR Quantitative Analysis of Human Red Blood Cell Proteome. J. Proteome Res 2017, 16 (8), 2752–2761. [PubMed: 28689405]

(62). Chu TTT; Sinha A; Malleret B; Suwanarusk R; Park JE; Naidu R; Das R; Dutta B; Ong ST; Verma NK; et al. Quantitative Mass Spectrometry of Human Reticulocytes Reveal Proteome-Wide Modifications during Maturation. Br. J. Haematol 2018, 180 (1), 118–133. [PubMed: 29094334]

(63). Wilson MC; Trakarnsanga K; Heesom KJ; Cogan N; Green C; Toye AM; Parsons SF; Anstee DJ; Frayne J Comparison of the Proteome of Adult and Cord Erythroid Cells, and Changes in the Proteome Following Reticulocyte Maturation. Mol. Cell. Proteomics 2016, 15 (6), 1938–1946. [PubMed: 27006477]

(64). Castagnola M; Messana I; Sanna MT; Giardina B Oxygen-Linked Modulation of Erythrocyte Metabolism: State of the Art. Blood Transfus. 2010, 8 (Suppl 3), s53–s58. [PubMed: 20606750]

(65). Kuhn V; Diederich L; Keller TCS; Kramer CM; Lückstadt W; Panknin C; Suvorava T; Isakson BE; Kelm M; Cortese-Krott MM Red Blood Cell Function and Dysfunction: Redox Regulation, Nitric Oxide Metabolism, Anemia. Antioxid. Redox Signaling 2017, 26 (13), 718–742.

(66). Liu H; Zhang Y; Wu H; D'Alessandro A; Yegutkin GG; Song A; Sun K; Li J; Cheng N-Y; Huang A; et al. Beneficial Role of Erythrocyte Adenosine A2B Receptor-Mediated AMP-Activated Protein Kinase Activation in High-Altitude Hypoxia. Circulation 2016, 134 (5), 405–421. [PubMed: 27482003]

(67). Reisz JA; Wither MJ; Dzieciatkowska M; Nemkov T; Issaian A; Yoshida T; Dunham AJ; Hill RC; Hansen KC; D'Alessandro A Oxidative Modifications of Glyceraldehyde 3- Phosphate Dehydrogenase Regulate Metabolic Reprogramming of Stored Red Blood Cells. Blood 2016, 128 (12), e32–42. [PubMed: 27405778]

(68). Hildebrandt T; Knuesting J; Berndt C; Morgan B; Scheibe R Cytosolic Thiol Switches Regulating Basic Cellular Functions: GAPDH as an Information Hub? Biol. Chem 2015, 396 (5), 523− 537. [PubMed: 25581756]

(69). D'Alessandro A; Nemkov T; Yoshida T; Bordbar A; Palsson BO; Hansen KC Citrate Metabolism in Red Blood Cells Stored in Additive Solution-3. Transfusion 2017, 57 (2), 325–336. [PubMed: 27813142]

(70). Brooks GA The Science and Translation of Lactate Shuttle Theory. Cell Metab. 2018, 27 (4), 757–785. [PubMed: 29617642]

(71). San-Millan I; Brooks GA. Reexamining Cancer Metabolism: Lactate Production for Carcinogenesis Could Be the Purpose and Explanation of the Warburg Effect. Carcinogenesis 2016, 38 (2), 119− 133.

(72). Tøien Ø; Drew KL; Chao ML; Rice ME Ascorbate Dynamics and Oxygen Consumption during Arousal from Hibernation in Arctic Ground Squirrels. Am. J. Physiol.-Regul. Integr. Comp. Physiol 2001, 281 (2), R572–R583. [PubMed: 11448862]

(73). Baumgartner R; Forteza MJ; Ketelhuth DFJ The Interplay between Cytokines and the Kynurenine Pathway in Inflammation and Atherosclerosis. Cytokine+ 2017, DOI: 10.1016/j.cyto.2017.09.004.

(74). Pierozan P; Biasibetti H; Schmitz F;Ávila H; Parisi MM; Barbe-Tuana F; Wyse ATS; Pessoa-Pureur R Quinolinic Acid Neurotoxicity: Differential Roles of Astrocytes and Microglia via FGF- 2-Mediated Signaling in Redox-Linked Cytoskeletal Changes. Biochim. Biophys. Acta, Mol. Cell Res 2016, 1863 (12), 3001–3014.

(75). Grant RS; Coggan SE; Smythe GA The Physiological Action of Picolinic Acid in the Human Brain. Int. J. Tryptophan Res 2009, 2, 71–79. [PubMed: 22084583]

(76). Culp-Hill R; Zheng C; Reisz JA; Smith K; Rachubinski A; Nemkov T; Butcher E; Granrath R; Hansen KC; Espinosa JM; et al. Red Blood Cell Metabolism in Down Syndrome: Hints on Metabolic Derangements in Aging. Blood Adv. 2017, 1 (27), 2776− 2780. [PubMed: 29296929]

(77). Canguilhem B; Miro JL; Kempf E; Schmitt P Does Serotonin Play a Role in Entrance into Hibernation? Am. J. Physiol 1986, 251 (4 Pt 2), R755–761.

(78). Chouchani ET; Pell VR; Gaude E; Aksentijevic D; Sundier SY; Robb EL; Logan A; Nadtochiy SM; Ord ENJ; Smith AC; et al. Ischaemic Accumulation of Succinate Controls Reperfusion Injury through Mitochondrial ROS. Nature 2014, 515 (7527), 431–435. [PubMed: 25383517]

(79). Chouchani ET; Pell VR; James AM; Work LM; Saeb Parsy K; Frezza C; Krieg T; Murphy MP A Unifying Mechanism for Mitochondrial Superoxide Production during Ischemia-Reperfusion Injury. Cell Metab. 2016, 23 (2), 254–263. [PubMed: 26777689]

(80). Bonora M; Wieckowsk MR; Chinopoulos C; Kepp O; Kroemer G; Galluzzi L; Pinton P Molecular Mechanisms of Cell Death: Central Implication of ATP Synthase in Mitochondrial Permeability Transition. Oncogene 2015, 34 (12), 1608–1608. [PubMed: 25790189]

(81). Tretter L; Patocs A; Chinopoulos C Succinate, an Intermediate in Metabolism, Signal Transduction, ROS, Hypoxia, and Tumorigenesis. Biochim. Biophys. Acta, Bioenerg 2016, 1857 (8), 1086–1101.

(82). Reisz JA; Wither MJ; Moore EE; Slaughter AL; Moore HB; Ghasabyan A; Chandler J; Schaub LJ; Fragoso M; Nunns G; et al. All Animals Are Equal but Some Animals Are More Equal than Others: Plasma Lactate and Succinate in Hemorrhagic Shock-A Comparison in Rodents, Swine, Nonhuman Primates, and Injured Patients. J. Trauma Acute Care Surg 2018, 84 (3), 537–541. [PubMed: 29112093]

(83). D'Alessandro A; Moore HB; Moore EE; Reisz JA; Wither MJ; Ghasasbyan A; Chandler J; Silliman CC; Hansen KC; Banerjee A Plasma Succinate Is a Predictor of Mortality in Critically Injured Patients. J. Trauma Acute Care Surg 2017, 83 (3), 491–495. [PubMed: 28590356]

(84). Desborough JP The Stress Response to Trauma and Surgery. Br. J. Anaesth 2000, 85 (1), 109–117. [PubMed: 10927999]

(85). Nemkov T; Sun K; Reisz JA; Yoshida T; Dunham A; Wen EY; Wen AQ; Roach RC; Hansen KC; Xia Y Metabolism of Citrate and Other Carboxylic Acids in Erythrocytes As a Function of Oxygen Saturation and Refrigerated Storage. Front. Med 2017, DOI: 10.3389/fmed.2017.00175.

(86). Kasmi KCE; Vue PM; Anderson AL; Devereaux MW; Ghosh S; Balasubramaniyan N; Fillon SA; Dahrenmoeller C; Allawzi A; Woods C; et al. Macrophage-Derived IL-1β/NF-KB Signaling Mediates Parenteral Nutrition-Associated Cholestasis. Nat. Commun 2018, 9 (1), 1393. [PubMed: 29643332]

(87). Blackstone E H2S Induces a Suspended Animation-Like State in Mice. Science 2005, 308 (5721), 518–518. [PubMed: 15845845]

(88). Elrod JW; Calvert JW; Morrison J; Doeller JE; Kraus DW; Tao L; Jiao X; Scalia R; Kiss L; Szabo C; et al. Hydrogen Sulfide Attenuates Myocardial Ischemia-Reperfusion Injury by Preservation of Mitochondrial Function. Proc. Natl. Acad. Sci. U. S.A 2007, 104 (39), 15560–15565. [PubMed: 17878306]

(89). Pryor WA; Houk KN; Foote CS; Fukuto JM; Ignarro LJ; Squadrito GL; Davies KJA Free Radical Biology and Medicine: It's a Gas, Man! Am. J. Physiol. Regul. Integr. Comp. Physiol 2006, 291 (3), R491–511. [PubMed: 16627692]

(90). Vandiver MS; Snyder SH Hydrogen Sulfide: A Gasotransmitter of Clinical Relevance. J. Mol. Med 2012, 90 (3), 255–263. [PubMed: 22314625]

(91). Wang R Physiological Implications of Hydrogen Sulfide: A Whiff Exploration That Blossomed. Physiol. Rev 2012, 92 (2), 791− 896. [PubMed: 22535897]

(92). Bekaert M; Edger PP; Hudson CM; Pires JC; Conant GC Metabolic and Evolutionary Costs of Herbivory Defense: Systems Biology of Glucosinolate Synthesis. New Phytol. 2012, 196(2), 596–605. [PubMed: 22943527]

(93). Salek RM; Steinbeck C; Viant MR; Goodacre R; Dunn WB The Role of Reporting Standards for Metabolite Annotation and Identification in Metabolomic Studies. GigaScience 2013, 2, 13. [PubMed: 24131531]

(94). Teufel R; Mascaraque V; Ismail W; Voss M; Perera J; Eisenreich W; Haehnel W; Fuchs G Bacterial Phenylalanine and Phenylacetate Catabolic Pathway Revealed. Proc. Natl. Acad. Sci. U. S.A 2010, 107 (32), 14390–14395. [PubMed: 20660314]

(95). Stanton TL; Sartin NF; Beckman AL Changes in Body Temperature and Metabolic Rate Following Microinjection of Met Enkephalinamide in the Preoptic/Anterior Hypothalamus of Rats. Regul. Pept 1985, 12 (4), 333–343. [PubMed: 3867098]

(96). Benchetrit T; Fournie-Zaluski MC; Roques BP Relationship between the Inhibitory Potencies of Thiorphan and Retrothiorphan Enantiomers on Thermolysin and Neutral Endopeptidase 24.11 and Their Interactions with the Thermolysin Active Site by Computer Modelling. Biochem. Biophys. Res. Commun 1987, 147(3), 1034–1040. [PubMed: 3478046]

(97). Oneda H; Inouye K Interactions of Human Matrix Metalloproteinase 7 (Matrilysin) with the Inhibitors Thiorphan and R-94138. J. Biochem 2001, 129 (3), 429–435. [PubMed: 11226883]

(98). D'Alessandro A; Dzieciatkowska M; Peltz ED; Moore EE; Jordan JR; Silliman CC; Banerjee A; Hansen KC Dynamic Changes in Rat Mesenteric Lymph Proteins Following Trauma Using Label-Free Mass Spectrometry. Shock 2014, 42 (6), 509–517. [PubMed: 25243424]

(99). Barbara G; De Giorgio R; Stanghellini V; Corinaldesi R; Cremon C; Gerard N; Gerard C; Grady EF; Bunnett NW; Blennerhassett PA; et al. Neutral Endopeptidase (EC 3.4.24.11) Downregulates the Onset of Intestinal Inflammation in the Nematode Infected Mouse. Gut 2003, 52 (10), 1457–1464. [PubMed: 12970139]

(100). Nieves E; Tobon LF; Ríos DI; Isaza A; Ramírez M; Beltran, J. A.; Garzon-Ospina, D.; Patarroyo, M. A.; Gomez, A. Bacterial Translocation in Abdominal Trauma and Postoperative Infections. J. Trauma 2011, 71 (5), 1258–1261. [PubMed: 21502873]

(101). Hachisu M; Takahashi H; Hiranuma T; Shibazaki Y; Murata S Relationship between Enkephalinase Inhibition of Thiorphan in Vivo and Its Analgesic Activity. J. Pharmacobio-Dyn 1985, 8 (9), 701–710. [PubMed: 3910797]

(102). Stevens CW; Sangha S; Ogg BG Analgesia Produced by Immobilization Stress and an Enkephalinase Inhibitor in Amphibians. Pharmacol., Biochem. Behav 1995, 51 (4), 675–680. [PubMed: 7675842]

(103). Pell VR; Chouchani ET; Frezza C; Murphy MP; Krieg T Succinate Metabolism: A New Therapeutic Target for Myocardial Reperfusion Injury. Cardiovasc. Res 2016, 111, 134. [PubMed: 27194563]

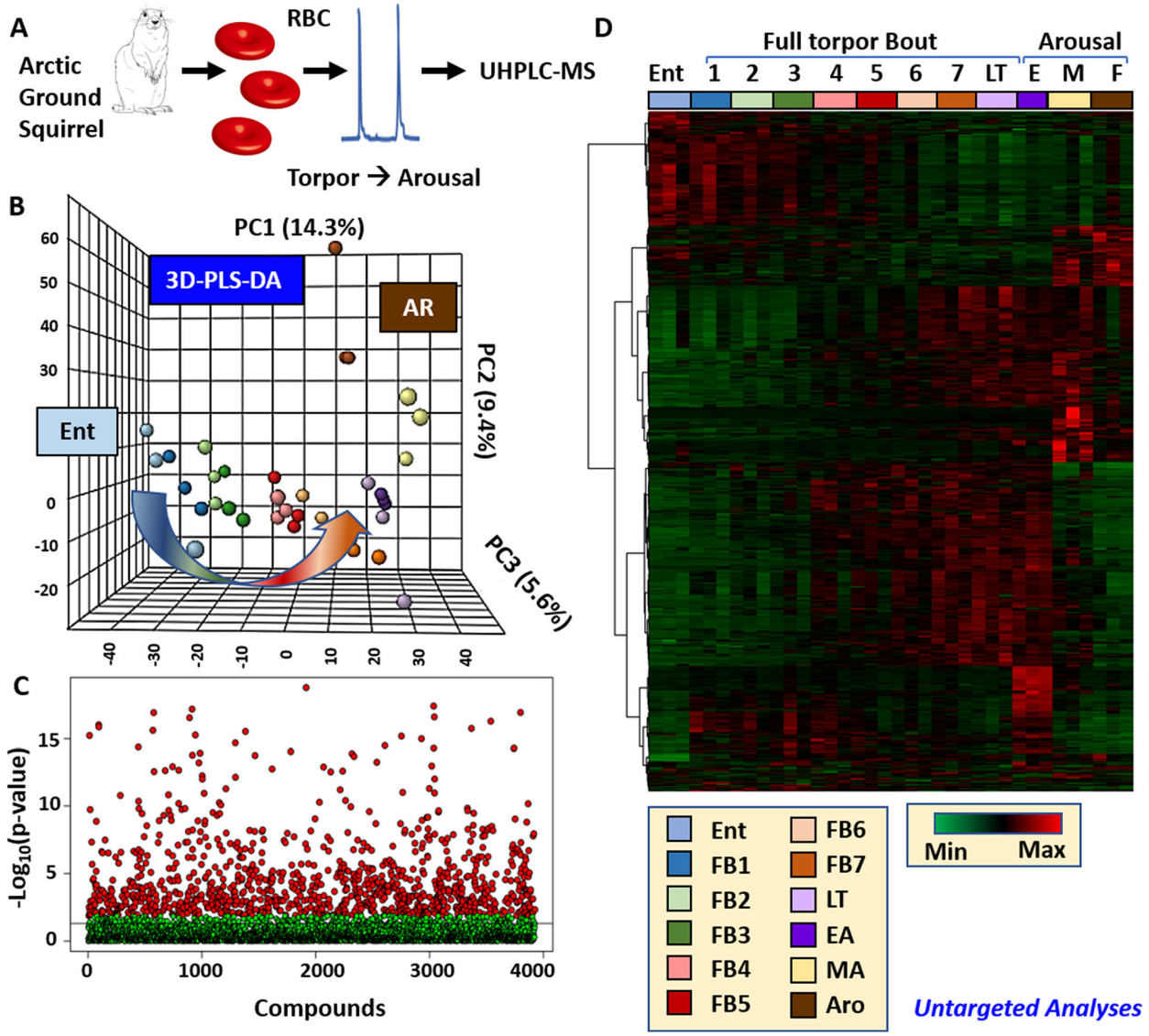

Figure 1.

Untargeted metabolomics of RBCs from arctic ground squirrels during torpor and arousal. An overview of the workflow is provided in A. A total of 3927 compounds were tentatively identified on the basis of intact and fragment mass, against the KEGG, Chemspider, NIST, and HMDB databases. Statistical analyses of untargeted metabolomics data in the form of partial least-squares-discriminant analysis (PLS-DA), Manhattan plots and hierarchical clustering analysis for the top 500 significant metabolites are shown in B, C, and D. A complete list of named metabolites is provided in the form of a table and figure in Table S1 and Figure S1.

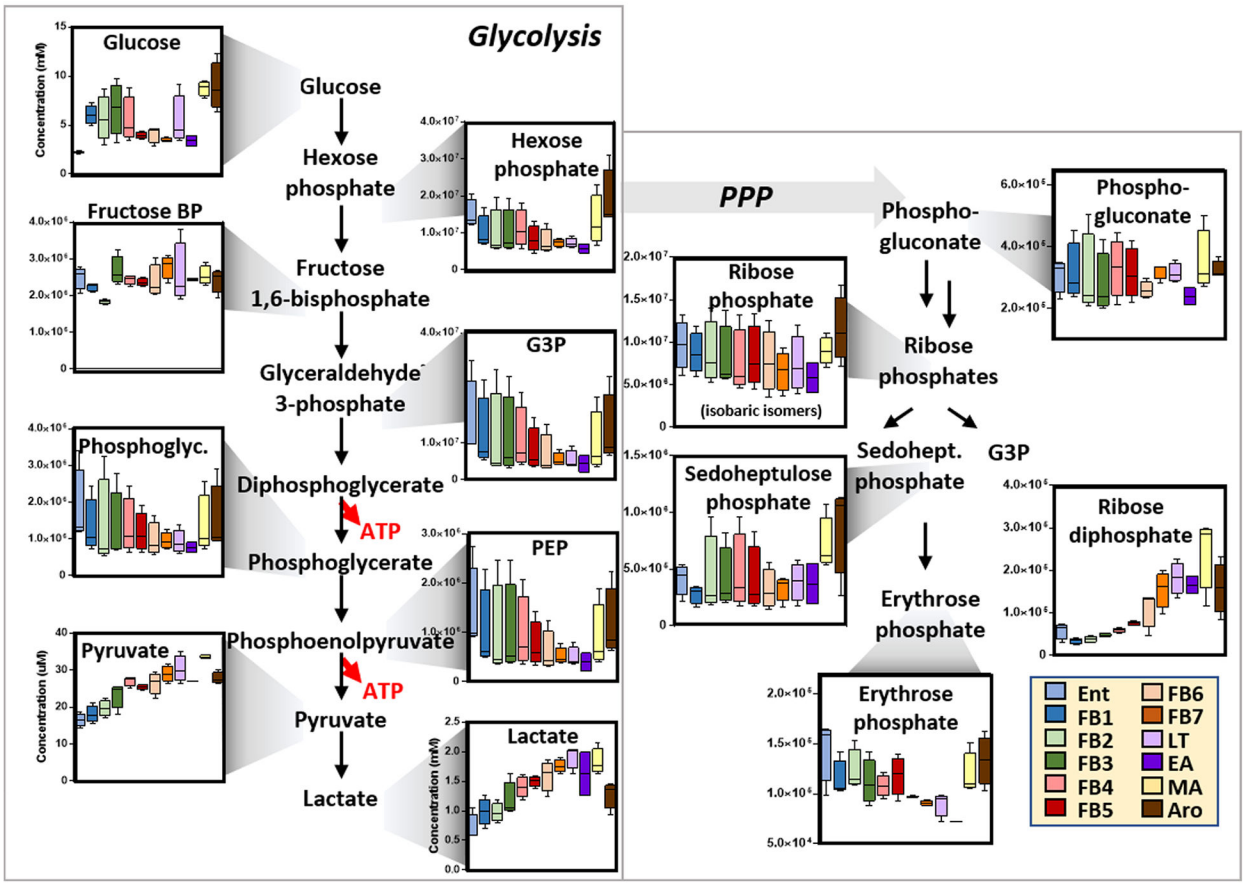

Figure 2.

An overview of glucose metabolism in RBCs from arctic ground squirrels during torpor and arousal. Box and whisker plots are shown. Color codes are used for the different phases, consistent with the legend.

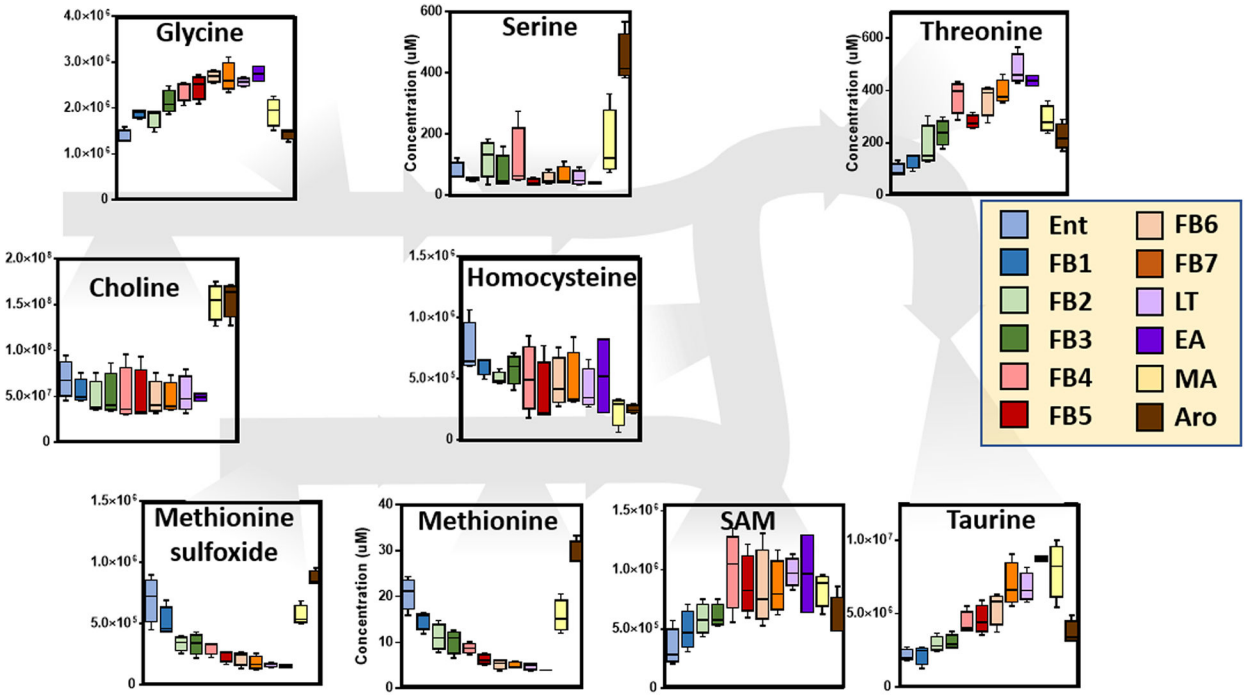

Figure 3.

An overview of one-carbon metabolism in RBCs from arctic ground squirrels during torpor and arousal. Box and whisker plots are shown. Color codes are used for the different phases, consistent with the legend.

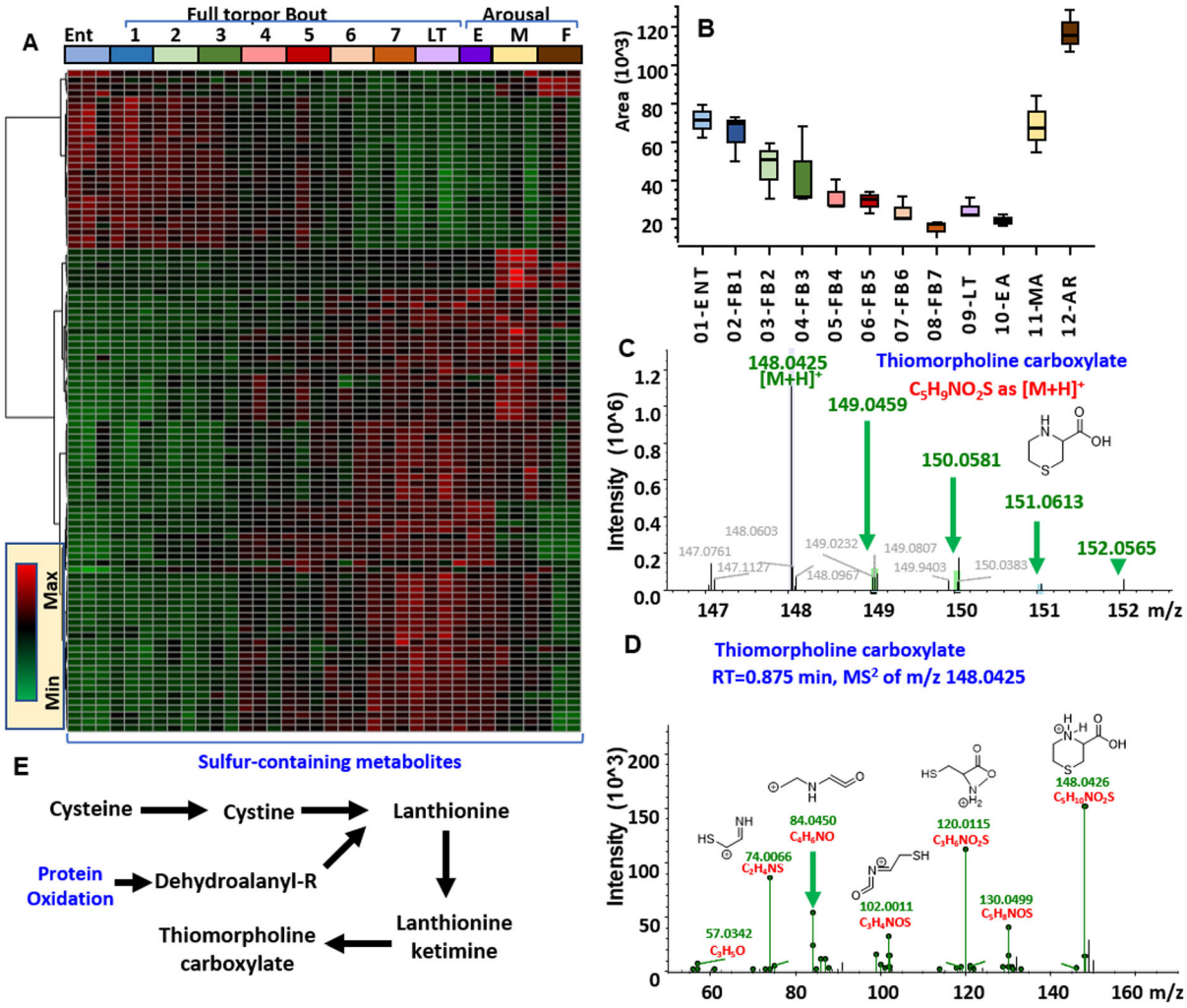

Figure 4.

Heat maps of sulfur-containing metabolites from untargeted metabolomics of RBCs from arctic ground squirrels during torpor and arousal (A). In B, C, and D, box and whisker plots, intact and fragment mass are provided for thiomorpholine carboxylate. In E, an overview of the pathways that can generate this metabolite in response to oxidative stress.

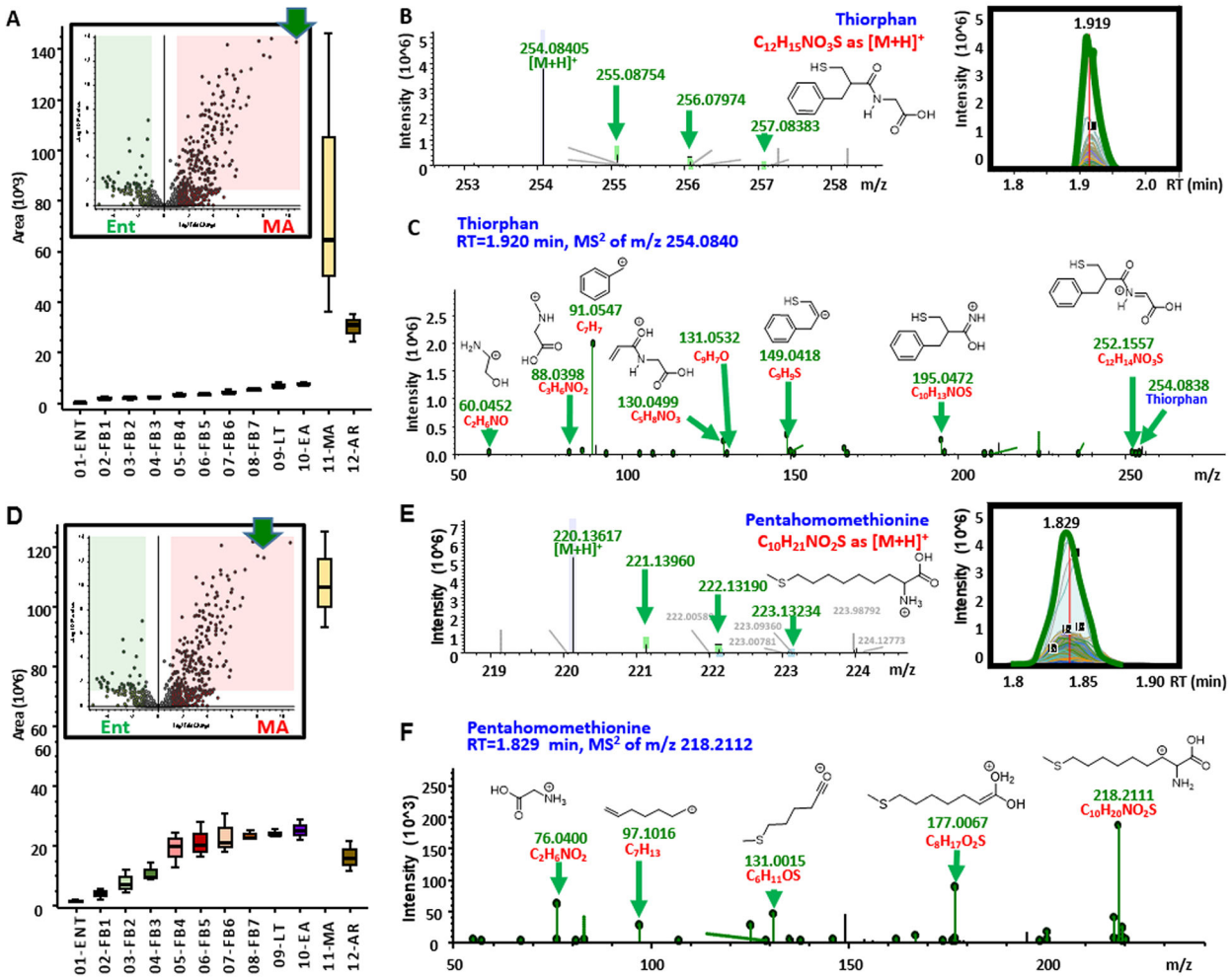

Figure 5.

Increase in sulfur containing metabolites during arousal in RBCs from arctic ground squirrels. From (A−C) and (D−F), box and whisker plots, intact and fragment mass are provided for thiorphan and pentahomomethionine. Fragmentation spectra in C and F are annotated with chemical formulas and structures as matched against the ChemSpider library.

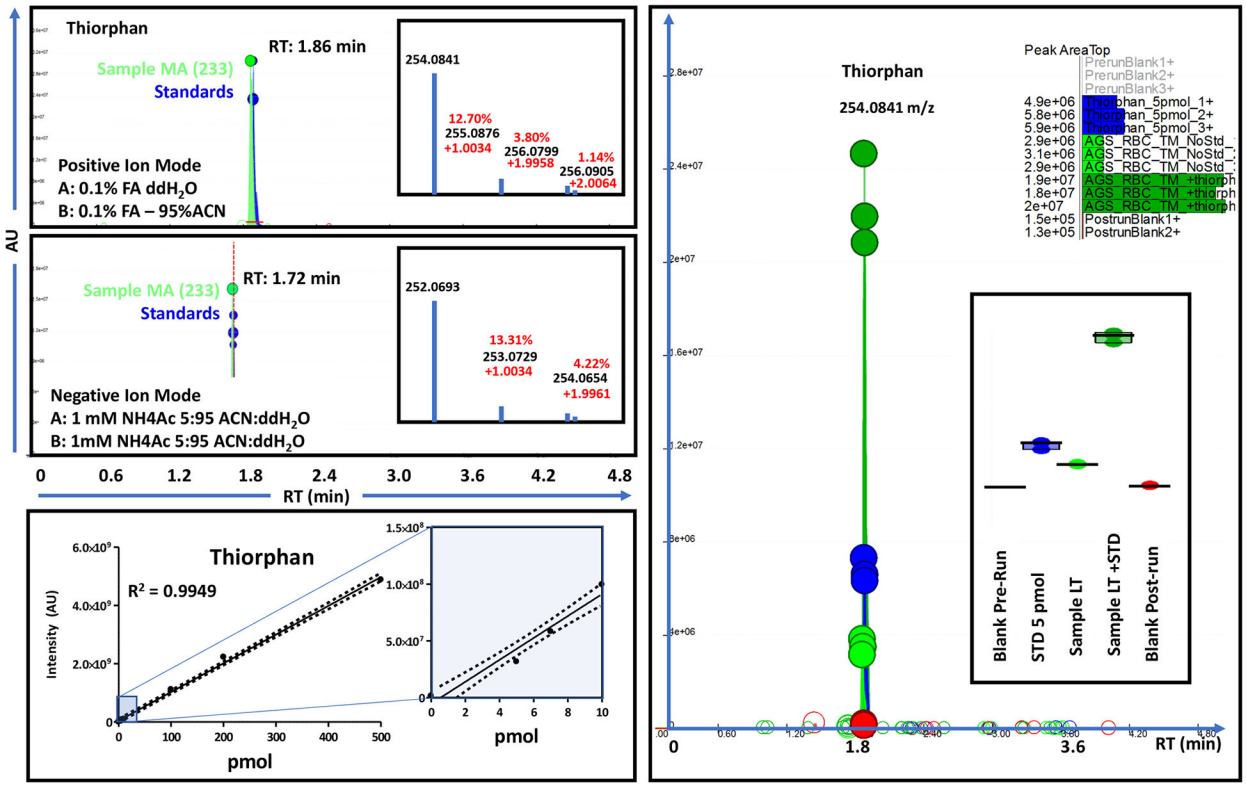

Figure 6.

Chromatographic runs for thiorphan standard (triplicate) and biological sample (middle arousal, MA, sample no. 233) in positive (top) and negative ion modes. Retention time changes between polarities result from different ion pairing agents in mobile phases across modalities. Calibration curve for thiorphan (bottom, from 5 to 500 pmol injected) and spike in addition of thiorphan (standard) into low thiorphan-containing late torpor samples (right-hand panel) are shown.

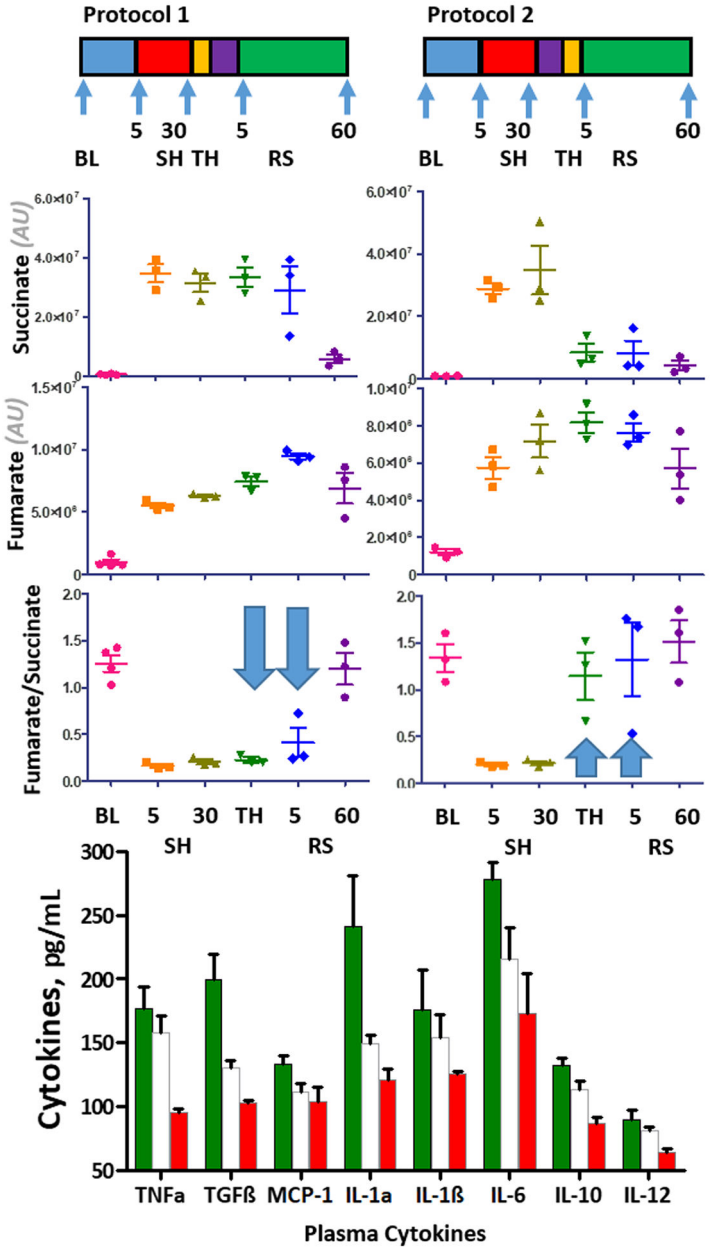

Figure 7.

Thiorphan injection (10 μM) prior to resuscitation in hemorrhaged rats prevents both reperfusion injury-like increases in fumarate/succinate ratios and the accumulation of plasma cytokines.